Specifying Local Oscillator Phase Noise Performance: How Good is Good Enough?

Robert Gilmore

Qualcomm, Inc.
10555 Sorrento Valley Road
San Diego, CA 92121
(619) 587 - 1121

Abstract

Definitive criteria are provided for specifying local oscillator phase noise performance for use in communication systems. In the absence of such criteria, many oscillators tend to be either under or over-specified. The emphasis is on digital modulation and demodulation, but analog communications are also considered. LO phase noise is analyzed for loss in demodulator performance, and also for impact on the modulation process. The results may be used to select an appropriate oscillator, or to tailor the noise characteristics of a frequency synthesizer design.

I. Introduction

The systems designer must consider the effects of local oscillator phase noise when planning a communication system. The effect of imperfect local oscillators is to degrade both the demodulation and modulation processes. The extent of the degradation depends upon the characteristics of the phase noise, and also upon the particular modulation type selected. It will be shown that LO phase noise may degrade a system in three major ways: a coherence error, a signal loss due to PM spreading, and an additive noise effect. The coherence error applies only to coherent digital demodulators. The other two effects apply to most receivers, but it will be shown that coherent BPSK is largely immune to the additive noise effect.

The paper begins with a description of pertinent concepts and definitions. The performance loss due to phase noise is described in general, and then specifically applied to the following demodulators: analog FM, non-coherent FSK, coherent BPSK, QPSK, OQPSK, and MSK, and differential PSK. Since phase noise may be specified either in the frequency or the time domain, some results are provided both in terms of frequency and time domain criteria. The emphasis is not upon the source of noise in oscillators, but rather upon the performance loss attributable to phase noise.

II. Definitions and Concepts

i. Fourier frequency

The frequency difference between a specific frequency component and the fundamental frequency (ie., the carrier) of a signal.

ii. $S_\phi(f)$

The one-sided spectral density of the phase fluctuations. Phase fluctuations are due to noise, instability, and modulation. The range of Fourier frequency f is from zero to infinity, and the dimensions are radians^2/Hz. $S_\phi(f)$ involves no power measurement of the signal - it is not a *power* spectral density which would be measured in Watts/Hz. In practice, $S_\phi(f)$ is measured by passing the signal through a phase detector and measuring the power spectral density at the detector output. (see Ref. 4)

iii. $\mathcal{L}(f)$

The normalized frequency domain representation of phase fluctuations. It is the ratio of the power spectral density in one phase modulation sideband, referred to the carrier frequency on a spectral density basis, to the total signal power, at Fourier frequency f. The units are 1/Hz. The frequency ranges from $-f_0$ to $+\infty$, where f_0 is the carrier frequency. $\mathcal{L}(f)$ is a 2-sided spectral density. For small angles ϕ (see Ref. 3),

$$\mathcal{L}(f) = S_\phi(f)/2 \qquad (1)$$

iv. $S_y(f)$

The spectral density of frequency fluctuations. In practice, $S_y(f)$ is measured by applying the signal to an FM detector and measuring the resulting spectral density. The dimensions are (fractional frequency)^2/Hz, or 1/Hz. The range of f is from zero to infinity. Since the random process $S_\phi(f)$ is differentiated to yield Sy(f) ,

$$S_y(f) = \left(\frac{f}{f_0}\right)^2 S_\phi(f) \qquad (2)$$

where f_0 is the carrier frequency.

v. Allan (or Pairwise) variance $\sigma^2(2,\tau)$

The instantaneous frequency of an oscillator is not observable since any measurement technique requires a finite time interval to be performed. We define $\overline{y}_k$ as a normalized frequency measurement over the gate time τ. Note that

$$\overline{y}_k = \frac{\phi(t_k+\tau) - \phi(t_k)}{2\pi f_0 \tau} \qquad (3)$$

Due to the random phase fluctuations of real oscillators, repeated measurements of $\overline{y}_k$ yield different results. The variance of this statistical process provides a time-domain measure of instability over τ. Assuming that the $\overline{y}_k$ have zero mean, the true variance is equal to

$$\sigma^2 [\overline{y}_k] = \langle \overline{y}_k^{\,2} \rangle \qquad (4)$$

where the bracket <> indicates a statistical average calculated over an infinite number of samples at a given time t_k. The Allan or pairwise variance is defined as:

$$\sigma_y^{\,2}(\tau) = \frac{1}{2} \langle (\overline{y}_2 - \overline{y}_1)^2 \rangle \qquad (5)$$

y_1 and y_2 are two adjacent samples taken τ seconds apart, hence *pairwise* variance. A practical measurement technique which involves M individual normalized frequency measurements $y_k = f_k/f_0$ results in the following widely accepted estimate of the Allan variance:

$$\sigma_y^{\,2}(\tau) = \frac{1}{2\,(M-1)} \sum_{k=1}^{M-1} (\overline{y}_{k+1} - \overline{y}_k)^2 \qquad (6)$$

vi. Power Low Noise Processes

Power low noise processes are models of oscillator noise that result in a particular slope of the spectral density verses frequency. The following table summarizes the five commonly identified power law noise processes, detailing their frequency behavior and Allan variance. (see Ref. 4)

Process Name	S_ϕ proportional to	S_y proportional to	$\sigma_y^2(\tau)$ Allan Variance
Random-walk FM	f^{-4}	f^{-2}	$\frac{3f_n}{(2\pi\tau f_o)^2}$
Flicker FM	f^{-3}	f^{-1}	$\frac{1.038 + 3\ln(\omega_n\tau)}{(2\pi\tau f_o)^2}$
White FM	f^{-2}	flat	$\frac{1}{2\tau f_o^2}$
Flicker øM	f^{-1}	f	$\frac{2\ln 2}{f_o^2}$
White øM	flat	f^2	$\frac{(2\pi)^2\tau}{6f_o^2}$

Table I: Power Low Noise Processes

In the table above, $f_n = \omega_n/2\pi$ is the measurement system 3 dB bandwidth (the measurement should be within 3 dB from DC to f_n).

vii. One-sided vs. Two-Sided Spectral Densities

By convention, noise processes are defined as one-sided spectral densities, and on a per-Hz of bandwidth density basis. The total mean-square fluctuation of frequency is given by (Ref. 3):

$$\text{Total Variance} = \int_0^\infty Sy(f)\,df \tag{7}$$

In contrast, two-sided spectral densities are defined such that the range of integration is from $-\infty$ to $+\infty$. The total variance of frequency fluctuations is given by

$$\int_{-\infty}^{\infty} S_{2\text{-sided}}\,df = 2\int_0^\infty S_{2\text{-sided}}\,df = \int_0^\infty S_{1\text{-sided}}\,df \tag{8}$$

In terms of $\mathscr{L}(f)$, a good approximation for the signals under discussion is

$$\mathscr{L}(-f) = \mathscr{L}(f) \tag{9}$$

However, for special cases of pure PM or FM, as well as correlated combinations of AM and PM, the RF spectral density of the signal is not symmetrical. For pure AM, the power spectral density is strictly symmetrical.

viii. Coherent vs. Incoherent Demodulation

Digital waveform demodulators which estimate the carrier phase of received waveforms are called *coherent* demodulators. In effect, the receiver is phase locked to the received signal. Signal integration is performed with a *phase synchronous replica of the signal, maximizing received signal energy.* Demodulators for phase shift keying (PSK), frequency shift keying (FSK), and continuous phase modulation (CPM) including minimum shift keying (MSK) may use coherent techniques.

Noncoherent demodulators do not estimate the phase of the incoming signal. The advantage of noncoherent detection is reduced demodulator complexity, including reduced local oscillator phase noise requirements in some cases. The penalty is increased bit error rate (BER) for a given signal-to-noise ratio. Noncoherent demodulators may be used for differential PSK (DPSK), FSK, ASK, and CPM.

ix. Orthogonal and Antipodal Signalling

Binary waveforms which are the negative of each other, such as

$$\begin{aligned} S_1(t) &= A \quad 0 \le t \le T \quad \text{for binary "1"} \\ S_2(t) &= -A \quad 0 \le t \le T \quad \text{for binary "0"} \end{aligned} \tag{10}$$

are called antipodal signals. The bit error performance of antipodal signalling with coherent demodulation is:

$$P_B = Q\left(\sqrt{\frac{A^2T}{N_o/2}}\right) = Q\left(\sqrt{\frac{2E_b}{N_o}}\right) \tag{11}$$

where the average energy per bit is $E_b = A^2T$. Q(x) is the inverse cumulative Gaussian distribution function:

$$Q(x) = \frac{1}{\sqrt{2\pi}} \int_x^\infty \exp(-\lambda^2/2)\, d\lambda \tag{12}$$

In contrast, an example of unipolar signalling is

$$\begin{aligned} S_1(t) &= A \quad 0 \le t \le T \quad \text{for binary "1"} \\ S_2(t) &= 0 \quad 0 \le t \le T \quad \text{for binary "0"} \end{aligned} \tag{13}$$

The bit error performance for unipolar signalling with coherent demodulation is given by:

$$P_B = Q\left(\sqrt{\frac{(A/2)^2T}{N_o/2}}\right) = Q\left(\sqrt{\frac{A^2T/2}{N_o}}\right) = Q\left(\sqrt{\frac{E_b}{N_o}}\right) \tag{14}$$

where the average energy per bit is $E_b = A^2T/2$ (the peak energy per bit, however, is A^2T).

Orthogonal signal sets are defined by

$$\int_0^T S_j(t)\, S_k(t)\, dt = A_j \delta_{jk} \qquad 0 \le t \le T \qquad j,k=1,\ldots,N \tag{15}$$

where $\delta_{jk} = \begin{cases} 1 \text{ for } j = k \\ 0 \text{ for } j \ne k \end{cases}$, A_j are constants

In the case of binary orthogonal waveforms, the distance between $S_1(t)$ and $S_2(t)$ in signal space is $\sqrt{2}A$, where $S_1(t)$ and $S_2(t)$ each have magnitude A. The probability of bit error for coherent demodulation is given by

$$P_B = Q\left(\sqrt{\frac{\left(\frac{\sqrt{2}\,A}{2}\right)^2 T}{N_o/2}}\right) = Q\left(\sqrt{\frac{A^2T}{N_o}}\right) = Q\left(\sqrt{\frac{E_b}{N_o}}\right) \tag{16}$$

where the average energy per bit is $E_b = A^2T$.

A vector-space representation of binary antipodal, unipolar, and orthogonal signalling is shown in Figure 1.

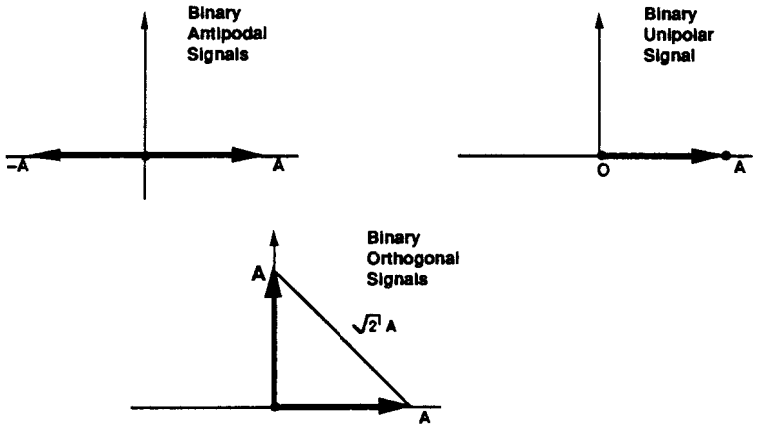

Figure 1: Binary Antipodal, Unipolar, and Orthogonal Signalling

Binary phase shift keying (BPSK) is an example of antipodal signalling. On-off keying (OOK) is an example of unipolar signalling. Frequency shift keying (FSK) is an example of orthogonal signalling if the tones are spaced at 1/T Hz for noncoherent detection or 1/2T Hz for coherent detection (Ref. 11). The E_b/N_0 performance difference between binary FSK (BFSK) and BPSK can be explained by the following argument. In the case of BFSK, the outputs of two detectors are compared for the presence of signal. At a given instant, one detector outputs signal plus noise while the other detector outputs noise only. Subtracting the two detector outputs yields +A for a one or -A for a zero. However, if the noise is independent in the two channels (i.e, white noise at different frequencies), the noise variances add. The noise power is doubled by subtracting the two detector outputs. Since the signal is bipolar, the signal is identical to the antipodal case, but the noise is 3 dB worse. Therefore, coherent BFSK performs 3 dB worse than coherent BPSK in AWGN.

x. The Relationship Between Phase Noise and Thermal Noise Density

Phase noise and thermal noise (i.e., AWGN) have important similarities and equally important differences. The similarites permit the system designer to add phase noise and thermal noise densities. A common way to ensure that phase noise will not impact system performance is to specify the phase noise density to be x dB (typically 20 dB) below the receive thermal noise density. The differences must be considered, however, in an accurate calculation of performance loss due to phase noise.

The major difference is that phase noise is a small angle random phase modulation of the received signal itself. In this regard, phase noise is more of a multiplicative effect than an additive process. The random PM process responsible for phase noise spreads the signal energy, and therefore reduces the signal power which carries useful information. Fortunately, this reduction in signal power is usually small. It is important to understand that phase noise is not added to the received signal, it is actually derived from the received signal by PM spreading.

When a carrier with a pedestal of pure phase noise power is downconverted to baseband I and Q channels, the phase noise appears primarily in the Q channel (assuming small angle phase modulation). This will be shown in this section. Noncoherent demodulators, which cannot distinguish between received phases, cannot benefit from this phenomena. Coherent modulation with information in the I channel only, such as coherent BPSK, are tolerant of LO phase noise because of this effect.

We now discuss the similarities between phase noise and AWGN. Consider superposed double-sideband thermal noise with total power $2N_0$ added to a carrier. Robins has shown (Ref. 6) that the DSB noise power may be represented as 4 sidebands, upper and lower pure AM sidebands and upper and lower pure PM sidebands, each with power No/2. Therefore, narrowband AWGN is a composite of $\frac{1}{2}$ AM and $\frac{1}{2}$ PM noise processes.

This result is consistent with the familiar results of signal-to-noise ratios in bandpass limiters. As the input signal-to-noise ratio of a bandpass limiter is varied, the asymptotes of the output SNR are well documented (Ref. 2):

$$\frac{(S/N)_{out}}{(S/N)_{in}} \rightarrow 2 \quad (+3\,dB) \text{ as } (S/N)_{in} \rightarrow \infty \tag{17}$$

$$\frac{(S/N)_{out}}{(S/N)_{in}} \rightarrow \frac{\pi}{4} \quad (-1.05\,dB) \text{ as } (S/N)_{in} \rightarrow 0$$

The +3 dB asymptotic increase in SNR for large input SNR's is due to the limiter suppression of the AM component of the additive noise. *The remaining noise is the PM component, and accounts for precisely $\frac{1}{2}$ of the input narrowband noise).*

The fact that additive narrow-band thermal noise may be represented as half AM and half PM is important to a discussion of the effect of phase noise on communications system performance. Phase noise effects system performance in three major ways - it degrades the coherence of the demodulation process, it reduces the signal power due to PM spreading, and it *adds noise.* Unlike thermal noise, additive phase noise due to local oscillators is typically non-white. However, the fact that additive thermal noise may be considered to be half phase noise implies that LO phase noise degrades the signal-to-noise ratio of a communications system as does thermal noise. The fact that LO phase noise is not flat, though, significantly complicates the calculation of performance degradation for this effect in contrast with additive white Gaussian noise (AWGN).

We now consider the integration of noise power over a frequency band. For thermal noise of power spectral density $N_o(f)$, the total power in an RF bandwidth $f_o \pm B$ is

$$P_N = \int_{-B}^{B} N_o(f)\, df \tag{18}$$

For white noise with power spectral density N_o over $f_o \pm B$,

$$P_N = 2N_oB \tag{19}$$

If we consider a clean carrier of power C at frequency f_o, we can calculate the phase jitter caused by additive noise power. Robins derives the modulation index of the phase modulation process $\theta \approx \sqrt{N_o/C}$ (ref 7, p. 22), and the RMS modulation index

$$\phi = \frac{\theta}{\sqrt{2}} \approx \sqrt{\frac{N_o}{2C}} \quad \text{radians} \tag{20}$$

The integrated phase jitter variance over $f_o \pm B$ is therefore given by

$$\overline{\phi^2} = \int_{-B}^{B} \frac{N_o(f)}{2C}\, df \quad \text{radians}^2 \tag{21}$$

If the noise is white,

$$\overline{\phi^2} = \frac{N_oB}{C} \quad \text{radians}^2 \tag{22}$$

and

$$\phi = \sqrt{\frac{N_oB}{C}} \quad \text{radians rms phase jitter} \tag{23}$$

Integrating pure phase noise with power spectral density $N_{LO}(f)$ over $f_o \pm B$ yields

$$P_N = \int_{-B}^{B} N_{LO}(f)\, df \tag{24}$$

Since $\mathcal{L}(f)$ is the normalized frequency domain measure of phase noise sidebands,

$$\mathcal{L}(f) = \frac{N_{LO}(f)}{C} \tag{25}$$

where C is the LO carrier power. The integrated phase jitter variance is given by Robins as

$$\overline{\phi^2} = \int_0^B \frac{2N_{LO}(f)}{C}\, df \qquad \text{radians}^2 \tag{26}$$

$$= \int_0^B 2\mathcal{L}(f)\, df \qquad \text{radians}^2 \tag{27}$$

For the case of white phase noise,

$$\overline{\phi^2} = \frac{2N_{LO}B}{C} \qquad \text{radians}^2 \tag{28}$$

and $$\phi = \sqrt{\frac{2N_{LO}B}{C}} \qquad \text{radians rms phase jitter} \tag{29}$$

Additional insight may be gained by considering the narrowband noise representation:

$$n(t) = x(t)\cos\omega_o t + y(t)\sin\omega_o t \tag{30}$$

where $\overline{x^2(t)} = \overline{y^2(t)} = \overline{n^2(t)} = N_o$

In polar coordinates,

$$n(t) = r(t)\cos[\omega_o t + \theta(t)] \tag{31}$$

where r(t) is Rayleigh distributed $0 \le r(t) \le \infty$
θ(t) is uniformly distributed $0 \le \theta(t) \le 2\pi$

This form shows the AM and PM portions of narrowband noise. If this noise process is downconverted to baseband using in-phase and quadrature local oscillators, the baseband portions of the I and Q downconverted outputs are

$$I(t) = \frac{r(t)}{2}\cos[\theta(t)] \tag{32}$$

$$Q(t) = \frac{-r(t)}{2}\sin[\theta(t)] \tag{33}$$

which are noise components each having equal power and θ(t) varying from 0 to 2π.

If a carrier is inserted into equation 30 the result is:

$$\begin{aligned} n(t) &= [x(t) + A]\cos\omega_o t + y(t)\sin\omega_o t \\ &= r(t)\cos[\omega_o t + \theta(t)] \end{aligned} \tag{34}$$

where r(t) is Rician distributed $0 \le r(t) \le \infty$ and θ(t) is an angle modulation process symmetrically distributed about 0° phase. In this case θ(t) is measured relative to the carrier. For small θ(t),

$$I(t) \approx \frac{r(t)}{2}\left(1 + \frac{\theta^2}{2}\right) \approx \frac{r(t)}{2} \tag{35}$$

$$Q(t) \approx \frac{-r(t)}{2}\theta(t) \tag{36}$$

The baseband I component contains primarily AM noise, and the Q component contains AM and PM noise. Therefore, the hard-limited Q channel provides a measure of the phase noise ($2\mathcal{L}(f) \approx S_\phi(f)$) of an oscillator. In the case of a carrier with pure phase noise, most of the downconverted phase noise appears in the Q channel if the small angle assumption is valid.

We conclude this section with a note of caution about noise calculations and measurements. When calculating or measuring the effects of phase noise, there are numerous possibilites of making 3 dB errors (Ref. 7, p. 37).

These include

a. One-sided vs. two-sided spectral densities. When integrating phase noise, plots of $S_\phi(f)$ or $2*\mathcal{L}(f)$ (that is, a plot of $\mathcal{L}(f)$ in dBc/Hz + 3 dB) must be used. A spectrum analyzer displays $\mathcal{L}(f)$, so 3 dB must be added when calculating the effects of phase noise.

b. Pure AWGN vs. phase noise.

c. Front-end limiting, which asymptotically may improve SNR in AWGN by 3 dB (or degrade it by 1.05 dB)

d. Measuring peak vs. RMS values.

e. SSB vs. DSB superposed AWGN.

III. General Formulation of the Problem

There are three major sources of communication system performance degradation due to LO phase noise:

1. Coherence or correlation error
2. Signal loss due to PM spreading
3. Additive noise effect

The degradation in signal to noise ratio is calculated for each effect (at the nominal receiver SNR in thermal noise) and the results are added in dB. There is also a small effect of phase noise on the demodulator bit timing loop, but this is shown to negligible in general in Ref. 7 (p. 260).

Coherence error applies to coherent demodulation only. Noise in the demodulator carrier tracking loop (i.e., phase noise estimation loop) causes a phase error which results in a loss in BER performance. The usual assumption is that the bandwidth of the phase estimation loop is small in comparison with the data rate. The resultant phase error may then be considered as constant during each bit interval. In an M-ary transmission with M > 2, this effect also produces interchannel interference. Demodulator phase error causes a cross coupling between, for example, the two orthogonal channels of a QPSK transmission. Coherence loss and interchannel interference will be discussed in detail in the following section.

The third effect is the increase in received noise floor due to the LO noise characteristics. LO noise is integrated in the detection bandwidth and added to integrated thermal noise:

$$\text{Total Noise Power} = \int_0^B N_{LO}\,df + \int_0^B N_o\,df \tag{37}$$

where N_{LO} is the one-sided noise spectral density due to the LO and N_0 is the one-sided thermal noise spectral density. From section II – x,

$$\mathcal{L}(f) = \frac{N_{LO}(f)}{C} \tag{38}$$

where C is the LO carrier power. The degraded signal-to-noise ratio in the detection bandwidth is then given by

$$\text{SNR} = \left[\int_0^B 2\mathcal{L}(f)\,df + \int_0^B \frac{N_O(f)}{C}\,df \right]^{-1} \tag{39}$$

where C is the LO carrier power.

A convenient way to evaluate the contribution of LO phase noise to total noise density is to plot the normalized phase noise density $\mathcal{L}(f)$ in dBc/Hz on the same plot as $\int^{B} 2\mathcal{L}(f)\,df$ in dBc. The lower integration limit is the phase estimation loop noise bandwidth for the case of coherent demodulation. This is because the phase tracking loop removes phase fluctuations within this frequency region (resulting in coherence error, as described in the following section). In the case of non-coherent demodulation, some high-pass lower limit is generally assumed (perhaps on the order of 1 Hz). An example is shown in Fig 2. Such a plot is easy to create using a computer spreadsheet program. Measured or predicted phase noise data is entered manually in one column, numerically integrated in another column, and both columns are plotted. 3 dB must be added to phase noise data measured on a spectrum analyzer to yield $2\mathcal{L}(f)$. Other spectrum analyzer corrections must usually be applied as well to correct for averaging in LOG mode, and for the envelope detector response to noise.

The integrated phase noise in dBc is compared with the signal-to-noise ratio at a particular frequency. In a digital communication system, the integrated phase noise is compared with E_b/N_o at f = bit rate. Note that

$$\frac{E_b}{N_o} = \frac{P_s \times R^{-1}}{N_o} = \frac{P_s}{N_o R} \qquad \text{dBc in BW} = R \tag{40}$$

where R = bit rate and N_o is assumed to be white. Therefore, E_b/N_o is the total signal power to $\int_0^{B} N_o\,df$ ratio, where thermal noise is integrated over a bandwidth equal to the bit rate. The integrated phase noise may be compared directly with E_b/N_o at $f = R$.

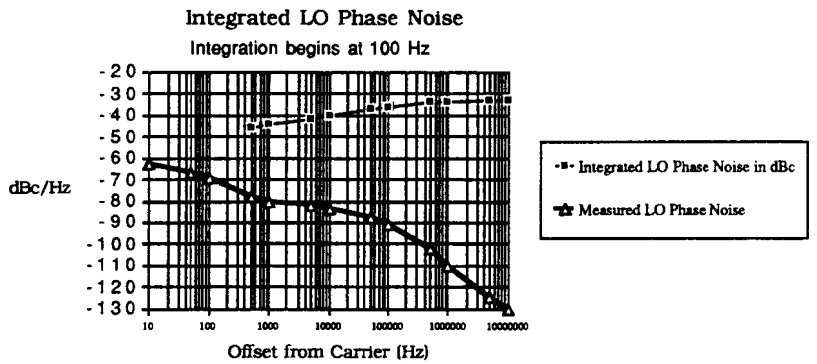

Figure 2: Example LO Phase Noise and Integrated Phase Noise Plot

Consider a 100 Kb/sec received signal data rate, and a nominal receiver operating E_b/N_o of 10 dB. Using the LO depicted in Fig 2, the integrated phase noise at 100 Kb/sec is -36 dBc. The integrated phase noise is 26 dB below thermal noise at the operating point. Summing a noise power X with a noise power X – ΔN dB yields a noise power X + Δ where

$$\Delta\,\text{dB} = 10 \log \left[1 + 10^{-\Delta N/10}\right] \tag{41}$$

For ΔN = 26 dB, Δ dB = 0.025. At this operating point, the LO phase noise degrades the received E_b/N_o by 0.025 dB. For convenience, Equation 41 is plotted in Figure 3.

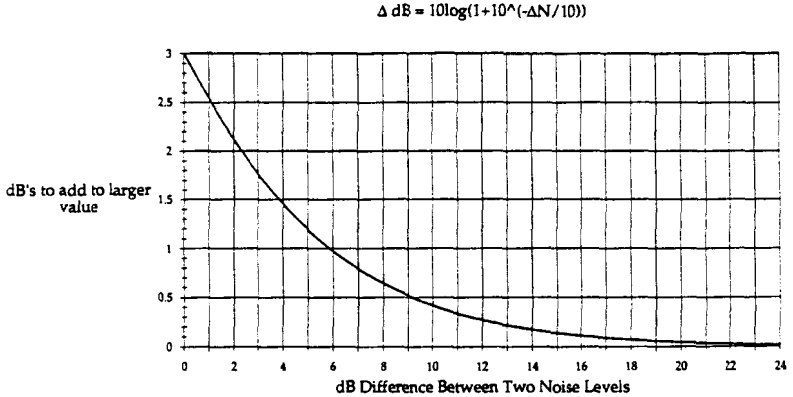

Figure 3: Addition of Two Noise Levels

This technique is straightforward, and added to the signal loss and coherence error effects provides a reasonable estimate of performance loss due to phase noise. For better accuracy though, each modulation type must be treated as a special case. The performance impact on specific modulation types is discussed in Section V.

In addition to being modulation specific, the performance degradation due to phase noise is implementation dependent. As has already been noted, it is easy to make 3 dB errors in these calculations. Unless painstaking attention is paid to analyzing a specific demodulator implementation, additional errors are possible. It is therefore recommended that sufficient margin be provided below the effects of thermal noise such that errors of a few dB are tolerable. An error of 3 dB with a margin of 20 dB is probably bearable, whereas a 3 dB calculation error with a margin of 10 dB may cause unacceptable performance.

IV. Coherence or Correlation Error

One effect of LO phase noise on coherent demodulation is that it causes a noisy estimate of phase. (Ref. 6). This results in a coherence or correlation performance degradation. This effect is also caused by additive thermal noise, and the phase noise contribution must be considered relative to thermal noise. Since phase noise tends to increase rapidly at small frequency offsets (typically f^{-3} behavior), phase noise may dominate over AWGN in the frequency region defined by the bandwidth of the phase estimation loop. In the case of M-ary transmissions where M > 2, coherence error results in inter-channel interference between the M-ary channels. The SNR degradation due to coherence error is added in dB to the degradation caused by the additive noise effect. The coherence error effect does not apply to non-coherent demodulators.

Coherent demodulation is performed by correlating the received signal with a phase reference derived by the phase estimation loop. If the bandwidth of the phase estimation loop could be made arbitrarily narrow, the phase noise and thermal noise jitter of the phase reference would be made negligible. System considerations, however, make this impractical. These include frequency instabilities, acquisition bandwidth requirements, and phase/frequency tracking requirements (due to doppler, etc.).

The bandwidth of the phase estimation loop is assumed to be small relative to the bit rate. The resultant phase error may be considered constant during each bit interval. The bit error probability is calculated by averaging the probability of error conditional on phase $P(E|\phi)$ over the density function of the phase estimation error ϕ.

Noise in the phase estimation loop causes a voltage correlation loss of $\cos(\phi)$ for a phase estimation error ϕ. This is the total degradation for coherent FSK (orthogonal signalling) and BPSK (antipodal signalling). For QPSK (4-ary orthogonal signalling) interchannel interference proportional to $\sin(\phi)$ is caused by cross coupling between the ideally orthogonal signal components. During each QPSK symbol interval one channel has destructive cross-coupling interference while the other channel has constructive

interference. The conditional probability of bit error $P(E|\phi)$ is the arithmetic mean of the error performances for destructive and constructive interference. The coherence error and cross-coupling are shown graphically in Figure 4.

a. BPSK b. QPSK

Figure 4: Coherence Error for BPSK and QPSK

Offset QPSK and MSK signalling will also be considered for performance loss due to coherence error. In offset QPSK, the bit transitions for one channel are staggered to occur at the center of the bit duration for the other channel. This avoids the possibility of 180° transitions, which cause the envelope of filtered QPSK to momentarily go to zero. When a bit transition occurs in offset QPSK, the cross coupling changes sign at midbit of the other channel, so the interference during the first half of the bit interval is cancelled by interference of the opposite polarity during the second half of the bit. Therefore, $P(E|\phi)$ has a correlation loss of $\cos(\phi)$ when a bit transition takes place. If no transition occurs, the situation is identical to QPSK. $P(E|\phi)$ is therefore equal to the average of the performance for BPSK and QPSK given a probability of bit transition of $\frac{1}{2}$ (i.e., random data). The analysis of correlation error for MSK signalling is significantly more complicated, and the results will be quoted from Matyas in Ref. 5.

In summary, the probability of error conditional upon the phase estimation error ϕ is:

$$P_F(E|\phi) = Q\left[\sqrt{\frac{E_b}{N_o}}\cos\phi\right] \quad \text{for FSK} \tag{42}$$

$$P_B(E|\phi) = Q\left[\sqrt{\frac{2E_b}{N_o}}\cos\phi\right] \quad \text{for BPSK} \tag{43}$$

$$P_Q(E|\phi) = \tfrac{1}{2}\ Q\left[\sqrt{\frac{2E_b}{N_o}}(\cos\phi + \sin\phi)\right] + \tfrac{1}{2}\ Q\left[\sqrt{\frac{2E_b}{N_o}}(\cos\phi - \sin\phi)\right] \quad \text{for QPSK} \tag{44}$$

$$P_{OQ}(E|\phi) = \tfrac{1}{2}\ P_B(E|\phi) + \tfrac{1}{2} P_Q(E|\phi) \quad \text{for OQPSK} \tag{45}$$

The probability density function for the phase estimation error ϕ given a first-order PLL is given by Viterbi (Ref. 12, p. 90):

$$P(\phi) = \frac{\exp(\alpha\cos\phi)}{2\pi I_0(\alpha)} \qquad -\pi \le \phi \le \pi \tag{46}$$

where α is the SNR of the phase reference in the phase estimation loop bandwidth:

$$\alpha = \frac{A^2}{N_o B_L} \approx (\text{phase error variance})^{-1} \tag{47}$$

I_0 is the zeroth-order modified Bessel function. This is also a close approximation to $P(\phi)$ for a second-order PLL for large α (Ref. 12, p. 111).

The degraded probability of error is given by:

$$P(e) = \int_{-\pi}^{\pi} P(E,\phi)\, d\phi \tag{48}$$

where $P(E,\phi) = P(E|\phi)\, P(\phi)$

This is, for FSK, BPSK, QPSK, and OQPSK:

$$P_F(e) = \int_{-\pi}^{\pi} P_F(E|\phi)\, P(\phi)\, d\phi \qquad \text{FSK} \qquad (49)$$

$$P_B(e) = \int_{-\pi}^{\pi} P_B(E|\phi)\, P(\phi)\, d\phi \qquad \text{BPSK} \qquad (50)$$

$$P_Q(e) = \int_{-\pi}^{\pi} P_Q(E|\phi)\, P(\phi)\, d\phi \qquad \text{QPSK} \qquad (51)$$

$$P_{OQ}(e) = \int_{-\pi}^{\pi} P_{OQ}(E|\phi)\, P(\phi)\, d\phi \qquad \text{OQPSK} \qquad (52)$$

These are plotted in Figures 5 – 9 along with the MSK data calculated by Matyas (Ref. 5). Parametric curves are provided vs. the SNR in the phase estimation loop:

$$\text{SNR} = 10 \log(\alpha)\ \text{dB} \qquad (53)$$

The detection loss in dB is plotted vs. the SNR of the phase reference at E_b/N_o = 7 dB in Figure 10.

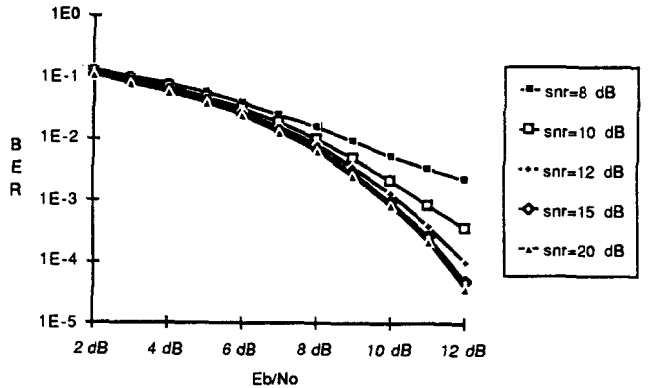

Figure 5: Coherent FSK Error Rate Performance vs. Tracking Loop SNR

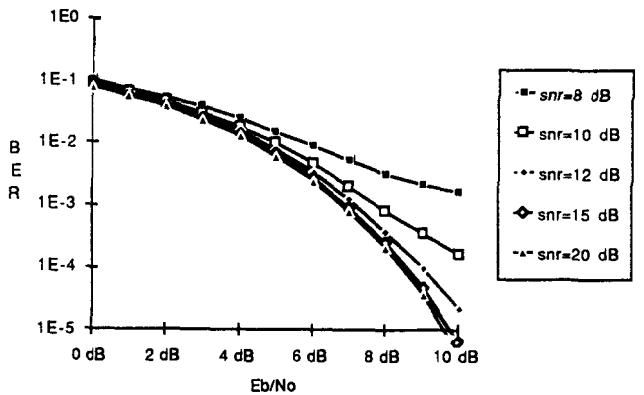

Figure 6: Coherent BPSK Error Rate Performance vs. Tracking Loop SNR

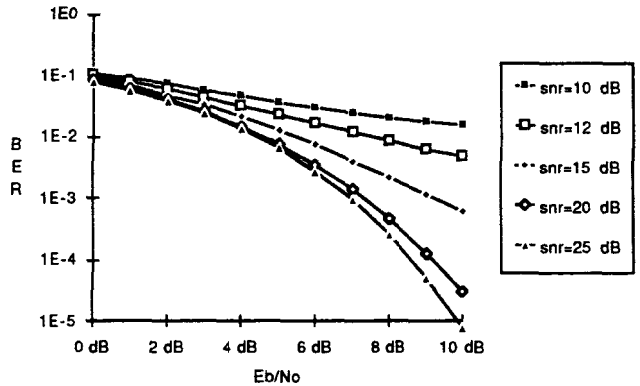

Figure 7: Coherent QPSK Error Rate Performance vs. Tracking Loop SNR

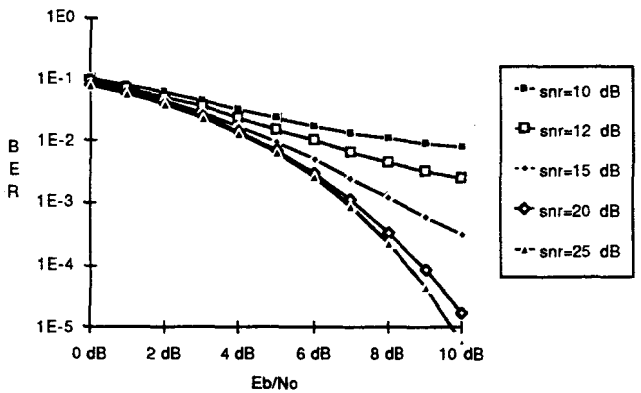

Figure 8: Coherent OQPSK Error Rate Performance vs. Tracking Loop SNR

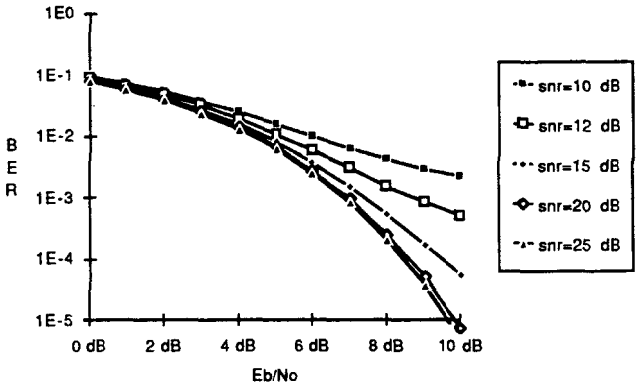

Figure 9: Coherent MSK Error Rate Performance vs. Tracking Loop SNR

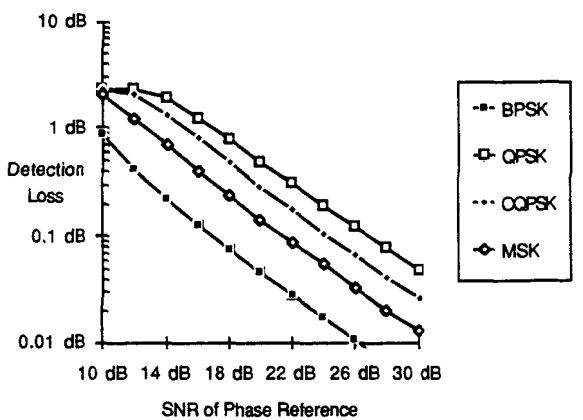

Figure 10: Detection Loss in dB vs. SNR of Phase Reference at E_b/N_o = 7 dB

Figs 5 – 10 may be used to establish the performance loss due to coherence error based on the SNR in the phase estimation loop bandwidth. They may also assist in the selection of the phase estimation loop bandwidth. The SNR in the loop bandwidth is given by

$$SNR = = \left[\int_0^{B_L} 2\mathcal{L}(f)\, df + \int_0^{B_L} \frac{N_o}{C}\, df \right]^{-1} \tag{54}$$

where B_L is the loop noise bandwidth, and N_o is the thermal noise spectral density.

V. Specific Cases

i. Analog FM

A frequency modulated carrier is described by

$$f_c(t) = A_c \cos\left[\omega_c t + 2\pi f_d \int^t m(\tau)\, d\tau \right] \tag{55}$$

where f_d is the frequency deviation. In the case of sinusoidal modulation,

$$f_c(t) = A_c \cos\left(\omega_c t + \beta \sin \omega_m t\right) \tag{56}$$

$$\beta = \frac{f_d}{f_m} = \text{modulation index} \tag{57}$$

where f_m is the modulating frequency. FM signals with $\beta < \pi/2$ are called narrowband FM. These signals have a spectrum with a large carrier plus smaller sidebands. FM signals with $\beta > \pi/2$ are called wideband FM, and exhibit a small carrier plus larger sidebands. The bandwidth of wideband FM signals increases rapidly as β is increased. The bandwidth of an FM signal with sinusoidal modulation is approximated by

$$B = 2 f_m (1 + \beta) \tag{58}$$

For arbitrary m(t) bandlimited to W Hz, this becomes Carson's rule:

$$B = 2 (f_d + W) \tag{59}$$

For small f_d (narrowband FM), the bandwidth is approximately 2W. For large f_d (wideband FM), the bandwidth is approximately 2 f_d.

The FM demodulater is shown in Figure 11.

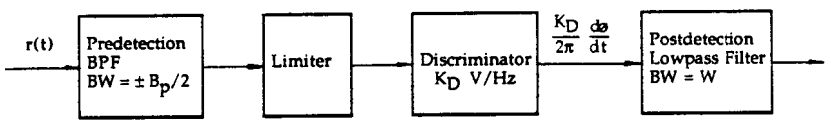

Figure 11: FM Demodulator

The limiter strips off AM noise, so that all noise in the demodulation process (either thermal, or due to LO phase noise) is PM. We first consider the case of AWGN only. The input to the demodulator is given by

$$r(t) = A_c \cos\left(\omega_c t + \phi(t)\right) \tag{60}$$

where $\phi(t) = 2\pi f_d \int^t m(\tau)\, d\tau$

plus AWGN of 2-sided spectral density $N_o/2$. The output of the predetection filter is

$$\begin{aligned} V(t) &= A_c \cos\left(\omega_c t + \phi(t)\right) + n_c(t) \cos(\omega_c t) - n_s(t) \sin(\omega_c t) \\ &= A_c \cos\left(\omega_c t + \phi(t)\right) + r_n(t) \cos\left(\omega_c t + \phi_n(t)\right) \end{aligned} \tag{61}$$

where $r_n(t)$ is Rayleigh distributed and $\phi_n(t)$ is uniformly distributed. For large SNR, the phase deviation of the discriminator input is (Ref. 15):

$$x(t) = \phi(t) + \frac{r_n(t)}{A_c} \sin\left[\phi_n(t) - \phi(t)\right] \tag{62}$$

Consider only noise through the demodulator ($\phi(t) = 0$). For $\phi(t) = 0$, $r_n(t) \sin\left[\phi_n t - \phi(t)\right] = n_s(t)$. The noise process at the discriminator output is

$$n(t) = \frac{k_D}{2\pi A_c} \frac{dn_s(t)}{dt} \tag{63}$$

Since the random process $n_s(t)$ is differentiated, the output power is given as

$$S_n(f) = \left(\frac{k_D}{2\pi A_c}\right)^2 \cdot (2\pi f)^2 N_o = \frac{k_D^2}{A_c^2} N_o f^2 \qquad \text{for } |f| < B_p/2 \tag{64}$$

$$= 0 \qquad \text{elsewhere}$$

This noise spectrum at the discriminator output is plotted in Figure 12.

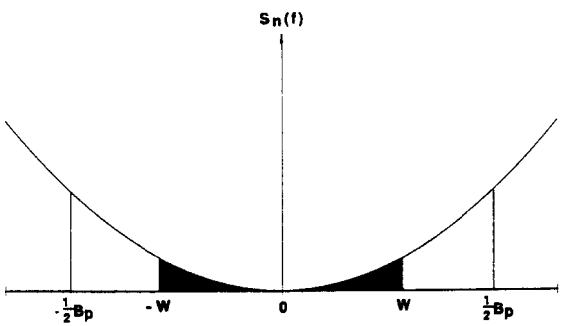

Figure 12: Noise Spectrum at FM Discriminator Output

Low frequency message signals are clearly subjected to lower noise levels than are high frequency signals. The output noise power after the postdetection filter is

$$P_N = \frac{k_D^2 2}{A_c^2} N_o \int_{-W}^{W} f^2 \, df = \frac{2 k_D^2 N_o W^3}{3A_c^2} = \frac{k_D^2 W^3}{3} \left(\frac{N_o}{C}\right)_t \tag{65}$$

where $(N_o/C)_t$ is the thermal noise to carrier power ratio.

The benefit of the postdetection lowpass filter is obvious. The predetection filter bandwidth B_p is greater than 2W. The output SNR is improved by the postdetection LPF of bandwidth W, which reduces the noise power but has no effect upon the signal. In practice, W must be somewhat greater than the signal bandwidth to prevent signal distortion. Note also that the output noise is inversely proportional to the carrier power $C = A_c^2/2$. As the carrier increases, the noise power drops. This is the well known FM "noise quieting" effect.

The SNR for FM systems operating above threshold is

$$\frac{S}{N} = \frac{3}{2W}\left(\frac{f_d}{W}\right)^2 \left(\frac{C}{N_o}\right)_t \qquad \text{for sinusoidal modulation} \tag{66}$$

$$\frac{S}{N} = \frac{3}{W}\left(\frac{f_d}{W}\right)^2 \left(\frac{C}{N_o}\right)_t \overline{m^2(t)} \qquad \text{for random modulation} \tag{67}$$

where $(C/N_o)_t$ is the SNR in thermal noise. It would appear that the SNR can be increased indefinitely by increasing the frequency deviation and therefore the bandwidth. The problem with this argument is that as the predetection bandwidth increases, more noise is applied to the limiter. When the noise power becomes greater than the signal power, it "captures" the limiter. This is the threshold effect. Below threshold, system performance deteriorates rapidly and the noise analysis above becomes invalid. The threshold level depends upon $(C/N_o)_t$ and (f_d/W). It is usually given as 10

dB for wideband FM. Note that this effect applies only to wideband FM. Narrowband FM ($f_d/W < \pi/2$) provides no SNR improvement over AM. The improvement is the consequence of restricting the phase deviations of the carrier caused by noise to small values, while maintaining large frequency variations due to the signal.

The FM detector's response to noise shown in Figure 12 shows the reason for the use of pre-emphasis and de-emphasis in FM systems. If higher frequencies are emphasized at the transmitter, they may be de-emphasized at the receiver prior to detection. The received noise at these higher frequencies is therefore reduced, compensating for the detector's parabolic sensitivity vs. frequency. If $H_{DE}(f)$ is the frequency response of the deemphasis filter, the output noise power is given by

$$N_D = \int_{-W}^{W} |H_{DE}(f)|^2 S_n(f)\, df \qquad (68)$$

where $S_n(f)$ is the input noise spectral density.

Now consider the effects of LO phase noise on the demodulation process. Two of the degradations described in Section III apply: signal loss due to PM spreading, and the additive noise effect. As described in Section III, LO phase noise is a random phase modulation of the signal itself, and therefore decreases the received signal power by the power in the phase noise sidebands. With the received signal power normalized to unity, the degraded signal power due to LO phase noise is:

$$P_D = 1 - \int_0^{\infty} S_{\phi}(f)\, df \qquad (69)$$

10 log (P_D) therefore gives this degradation in dB.

The second degradation is the added noise due to the LO in the region $0 \le f \le W$. The degradation due to this noise power being x dB below thermal noise is given in Figure 3 for C/N_0 values above the FM threshold. The requirement that phase noise power be a factor x below thermal power can be stated as

$$\int_0^W 2\mathcal{L}(f) f^2\, df \le \frac{1}{x}\left(\frac{N_o}{C}\right)_t \frac{W^3}{3} \qquad (70)$$

The right side of Eq. 70 is from Eq. 65. The discriminator constant k_D is taken to be unity, since it applies equally to both sides of Eq. 70. In practice, the integral on the left is evaluated from some highpass cutoff frequency f_h rather than 0. If a de-emphasis filter is used at the receiver, then Eq. 70 is modified as follows:

$$\int_{f_h}^W |H_{DE}(f)|^2 2\mathcal{L}(f) f^2 df \le \frac{1}{x}\left(\frac{N_o}{C}\right)_t \int_{f_h}^W |H_{DE}(f)|^2 f^2 df \qquad (71)$$

ii. Non-Coherent FSK

Coherent detection of FSK is rarely used in practice since it only yields approximately 1 dB of performance improvement over non-coherent detection. We therefore focus on non-coherently detected FSK.

Figure 13 is a block diagram for the MFSK demodulator.

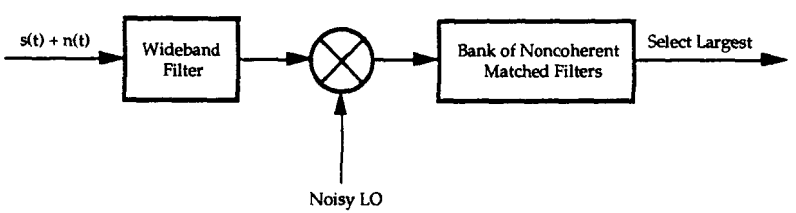

Figure 13: Noncoherent MFSK Demodulator

The matched filters each have a $\sin(\pi fT)/\pi fT$ response, where T is the bit duration. It is assumed that the transmitted signal is mixed down to the matched filter at zero Hz using an LO disturbed by the random phase modulation $\phi(t)$, having spectral density $S_\phi(f)$. The filters are spaced at the tone spacing f_s. Since the demodulator does not estimate received phase, the energy output of the correct filter must involve both the I and Q channels:

$$Y^2 = I^2 + Q^2$$

With the non-degraded correct filter output normalized to unity, the correct filter output power is given by (Ref. 13):

$$\overline{Y^2} = 1 - \sigma_\phi^2 + \int_0^\infty S_\phi(f) \left[\frac{\sin(\pi fT)}{\pi fT}\right] df$$

$$= 1 - \int_0^\infty S_\phi(f)\, df + \int_0^\infty S_\phi(f) \left[\frac{\sin(\pi fT)}{\pi fT}\right]^2 df$$

$$= 1 - \int_0^\infty \left[1 - \left(\frac{\sin(\pi fT)}{\pi fT}\right)^2\right] S_\phi(f)\, df \qquad (72)$$

For tones with orthogonal spacing $f_s = n/T$, the incorrect (noise only) filter outputs are given by

$$\overline{Y_N^2} = \int_0^\infty S_\phi(f) \left[\frac{\sin\pi(f - f_s)T}{\pi(f - f_s)T}\right]^2 df \qquad (73)$$

The correct filter output is equal to the uncorrupted signal power, minus the power in the phase noise sidebands, plus the power recovered in the filter. The incorrect filter outputs are simply the spectrum of the random phase process passed through the linear matched filters. For other than binary FSK, the noise contributions of each of the incorrect matched filters must be summed up. Each component is calculated by replacing f_s by nf_s in Eq. 73.

The resulting SNR is, where N = thermal noise power,

$$SNR = \frac{S \cdot \overline{Y^2}}{N + S \cdot \overline{Y_N^2}} = \frac{S \cdot \overline{Y^2}}{N\left(1 + \frac{S}{N} \cdot \overline{Y_N^2}\right)}$$

$$= \frac{S}{N} \cdot \frac{\overline{Y^2}}{1 + \frac{S}{N} \cdot \overline{Y_N^2}} \qquad (74)$$

The integrals in equations 72 and 73 may be evaluated numerically, and the degradation to the SNR in thermal noise is given by Eq. 74.

Charles Wheatley (Ref. 13) has analyzed the degraded signal power given by Eq. 72 for the case where

$$S_{\phi_i}(f) = \frac{k_i}{f^i} \qquad i = 0,1,2,3 \qquad (75)$$

That is, the power low processes that typically describe oscillator phase noise. He also provides approximate expressions for the loss factors $(1 - \overline{Y^2})$ in terms of the Allan variances of these processes, which were given in Section II – vi. The results are summarized in Table 2. Note that

$$\overline{Y^2} = 1 - \int_{f_1}^{f_2} \left[1 - \left(\frac{\sin(\pi fT)}{\pi fT}\right)^2\right] \frac{k_i}{f^i} df \qquad i = 0,1,2,\ldots \qquad (76)$$

Although the results in Table 2 are precise only for non-coherent FSK, they are useful in assessing the relative impact of phase noise in general. If the coefficients $k_0 - k_3$ are known, or Allan variance measurements are available, the results provide a quick, relative measure of phase noise impact.

Notes: f_1 = lower integration limit
f_2 = upper integration limit
T = bit duration
f_o = center frequency

Phase Noise $S_\phi(f)$	$\overline{Y^2}$	$1-\overline{Y^2}$ in terms of Allan variance
k_0	$1-k_0 f_2$	$\frac{(2\pi f_o T)^2}{3}\sigma_y^2(\tau)$
k_1/f	$1-k_1\left[\ln(2\pi f_2 T)+0.23\right]$	$\approx \frac{(2\pi f_o T)^2}{3}\sigma_y^2(\tau)$
k_2/f^2	$1-\frac{\pi^2 k_2 T}{3}$	$\frac{(2\pi f_o T)^2}{6}\sigma_y^2(\tau)$
k_3/f^3	$1-\frac{k_3\pi^2T^2}{3}\left[\ln(2\pi f_1 T)^{-1}\right]$	$\frac{(2\pi f_o T)^2\ln\left[(2\pi f_1 T)^{-1}\right]}{24\ln(2)}\sigma_y^2(\tau)$

Table 2: Signal Degradation for Integrate and Dump Matched Filters

Note that the signal degradation in dB is given by $10\log\left(\overline{Y^2}\right)$

iii. Coherent Demodulation of BPSK

The coherent BPSK demodulator is quite tolerant of local oscillator phase noise. Since BPSK is an antipodal waveform, the coherence loss due to phase reference SNR is significantly less than for M-ary PSK with M > 2. Another important consideration is that BPSK contains no information in the Q channel (the binary data is transmitted in phase with the carrier). It was shown in Section II-ix that for a small angle phase noise process, downconverted phase noise appears primarily in the Q channel. Therefore, BPSK does not have the additive noise degradation described in Section III. Most of the phase noise is orthogonal to the modulation, and is not seen by the demodulator. Since the phase estimation loop processes both the I and Q channels, the coherence loss effect is properly described in Section IV.

The SNR performance degradation due to phase noise is the sum in dB of the coherence loss defined in Section IV, plus the loss in signal power due to the PM spreading effect: $10\log\left(1-\int_0^\infty S_\phi(f)\,df\right)$dB.

iv. Coherent Demodulation of QPSK, OQPSK, MSK

Unlike the case of BPSK, each of these coherent demodulators processes information in both the I and Q channels. The SNR performance degradation due to LO phase noise is the sum in dB of the coherence loss, the PM spreading loss, and the additive noise loss. The LO phase noise spectrum is integrated as described in Section III, and found to be a factor x below the thermal noise power:

$$\int_{B_L}^{1/T} 2\,\mathcal{L}(f)\,df \le \frac{1}{x}\left(\frac{N_o}{C}\right)\frac{1}{T} \qquad (77)$$

where B_L is the phase estimation loop BW and T is the bit rate. The loss associated with a noise floor 10log(x) below thermal noise is derived from Figure 3. This is added to the coherence loss in dB from Section IV, plus the PM spreading loss $10\log\left(1-\int_0^\infty S_\phi(f)\,df\right)$dB.

v. Differential BPSK

Differential demodulation of PSK is typically used for low bit rate transmissions, which would require excellent LO phase noise close to the carrier for coherent demodulators. For example, a coherent demodulator for 100 bps would have a phase estimation loop bandwidth of 10 Hz or less. The phase noise within 10 Hz of the carrier would have to be low enough to assure coherence. The differential PSK demodulator measures the phase difference between two successive received bits rather than comparing each received bit with a derived phase reference. The resulting loss in bit error rate performance may be justified by the relaxed requirements upon LO phase noise.

Robins (Ref. 7) has shown that the differential phase detector has a sinusoidal sensitivity to noise. The integrated phase jitter variance is given by

$$\overline{\Delta\phi^2} = \int_0^{\frac{1}{T}} 2\left(\frac{N_o}{C}\right)_t \sin^2(\pi fT)\, df \qquad \text{thermal noise} \qquad (78)$$

$$= \int_0^{\frac{1}{T}} 2\,\mathcal{L}(f) \sin^2(\pi fT)\, df \qquad \text{LO phase noise} \qquad (79)$$

where T is the bit duration. For the case of white noise

$$\overline{\Delta\phi^2} = 2\left(\frac{N_o}{C}\right) \int_0^{\frac{1}{T}} \sin^2(\pi fT)\, df = \left(\frac{N_o}{C}\right)\frac{1}{T} \qquad (80)$$

Although the noise sensitivity has a $\sin^2(\pi fT)$ dependence on f, the integrated phase jitter variance for a *white noise* input may be calculated assuming the demodulator characteristic is flat from 0 – 1/T. For the phase noise contribution to be a factor x below thermal noise:

$$\int_0^{\frac{1}{T}} 2\,\mathcal{L}(f) \sin^2(\pi fT)\, df \le \frac{1}{x}\left(\frac{N_o}{C}\right)\frac{1}{T} \qquad (81)$$

Should the phase noise function not be well behaved in the neighborhood of 0 Hz, the lower integration limit may be taken as some low high-pass cutoff frequency f_h (a highpass filter of cut-off frequency ~ 1 Hz will have minimal impact on the demodulator).

The degradation due to phase noise is the loss due to the LO noise power 10log(x) dB below thermal noise as given in Figure 3, plus the loss in signal power due to the PM spreading effect: $10 \log\left(1 - \int_0^{\infty} S_\phi(f)df\right)$ dB. The LO noise power is computed using Equation 81.

VI. Effects on the Modulation Process

The signal loss due to PM spreading and the additive noise effect described in Section III apply to the modulator as well as the demodulator. The signal loss due to PM spreading at the modulator, $1 - \int_0^{\infty} S_\phi(f)\, df$, is not recoverable. The noise floor added by phase noise also cannot be improved by subsequent processing. It is interesting to note that a hard limiter placed after the upconverter has no effect upon pure phase noise. Therefore, the same performance criteria must be applied to the modulator LOs as well as those in the receiver. When computing the performance due to LO phase noise, the effects of all local oscillators in the system must be considered. These include the LOs in the transmitter, those in the receiver, and the LOs in any repeaters in the link.

VII. Conclusion

Criteria have been provided to calculate the effects of phase noise on communications system performance. The precise degradation has been given for non-coherent FSK, and techniques for calculating the effect on other modulation types have been described. A remaining task is to derive the precise analytical solution for these other modulation types.

Some tests for an adequate phase noise spectrum have been described which are relatively easy to perform. If the Allan variance or power-law process coefficients are known for an oscillator, the effect upon the signal assuming an ideal integrate and dump matched filter can be quickly derived from Table 2. This may be done for a quick check whether or not a particular LO is a concern. The phase noise integration technique described in Section III can be implemented quickly using a spreadsheet program, and gives an indication of the relative severity of the phase noise issue. Although somewhat more time consuming, summing each of the effects of coherence error, signal loss due to PM spreading, and the additive noise effect described in Sections III and IV provide an accurate prediction of performance with imperfect local oscillators.

VIII. Acknowledgement

The author wishes to thank Richard Kornfeld and Dr. Charles E. Wheatley III of QUALCOMM, Inc. for invaluable discussions on this topic, and the preparation of the plots in Section IV. Tremendous thanks are also due to Susana Anaya of QUALCOMM, Inc. for the preparation of the manuscript.

References

1. J. A. Barnes, et al, "Characterization of Frequency Stability," *IEEE Transactions on Instrumentation and Measurement*, Vol. IM-20, No. 2, May 1971, pp. 105-120

2. W. B. Davenport, "Signal-to-Noise Ratios on Band-Pass Limiters," *Journal of Applied Physics*, Vol. 24, No. 6, June 1953.

3. D. Halford, J. Shoaf, and A. S. Risley, "Spectral Density Analysis: Frequency Domain Specification and Measurement of Signal Stability," *Proceedings of the 27th Annual Symposium on Frequency Control, U. S. Army Electronics Command*, Fort Monmouth, New Jersey, June 1973, 11 pages

4. D. A. Howe, "Frequency Domain Stability Measurements: A Tutorial Introduction," Nat. Bur. Stand. (U.S.) Tech Note 679, March 1976, 27 pages

5. R. Matyas, "Effect of Noisy Phase References on Coherent Detection of FFSK Signals," *IEEE Transactions on Communications*, Vol. Com-26, N, June 1978, pp. 807-815

6. S. A. Rhodes, "Effect of Noisy Phase Reference on Coherent Detection of Offset-QSPK Signals," *IEEE Transactions on Communications*, Vol. Com-22, No. 8, Aug 1974, pp. 807-815

7. W. P. Robins, *Phase Noises in Signal Sources (Theory and Applications)*. IEE Telecommunications Series 9, Peter Peregrinus Ltd., London, UK., 1982

8. J. Rutman, "Characterization of Phase and Frequency Instabilities in Precision Frequency Sources: Fifteen Years of Progress," *Proceedings of the IEEE*, Vol. 66, No. 9, Sept 1978, pp. 1048-1075

9. J. H. Shoaf, D. Halford, and A. S. Risley, "Frequency Stability Specification and Measurement: High Frequency and Microwave Signals," Nat. Bur. Stand. (U.S.) Tech Note 632, Jan 1973, 70 pages

10. M. Schwartz, *Information Transmission, Modulation, and Noise.* McGraw-Hill, New York, N.Y., 1970

11. B. Sklar, *Digital Communications Fundamentals and Applications.* Prentice Hall, Englewood Cliffs, New Jersey, 1988

12. A. J. Viterbi, *Principals of Coherent Communication.* McGraw-Hill, New York, N.Y., 1966

13. C. E. Wheatley III, private notes.

14. J. M. Wozencraft and I. M. Jacobs, *Principals of Communication Engineering.* John Wiley & Sons, Inc., New York, N.Y., 1965

15. R. E. Ziemer and W. H. Tranter, *Systems, Modulation, and Noise.* Houghton Mifflin, Co., Boston. 1976